



Title	Helium thermal desorption and retention properties of V-4Cr-4Ti alloy used for first wall of breeding blanket
Author(s)	Hirohata, Y.; 廣畑, 優子; Yamada, T. et al.
Citation	Fusion Engineering and Design, 81(1-7), 193-198 <a href="https://doi.org/10.1016/j.fusengdes.2005.08.095">https://doi.org/10.1016/j.fusengdes.2005.08.095</a>
Issue Date	2006-02
Doc URL	<a href="https://hdl.handle.net/2115/5923">https://hdl.handle.net/2115/5923</a>
Type	journal article
File Information	FED81-1.pdf



## Helium thermal desorption and retention properties of V-4Cr-4Ti alloy used for first wall of breeding blanket

Y. Hirohata<sup>1)</sup>, T. Yamada<sup>1)</sup>, Y. Yamauchi<sup>1)</sup>, T. Hino<sup>1)</sup>, T. Nagasaka<sup>2)</sup> and T. Muroga<sup>2)</sup>

1) Hokkaido University, Kita-ku, Sapporo, Hokkaido, 060-8628 Japan

2) National Institute for Fusion Science, Toki, Gifu, 509-5292 Japan

Corresponding author: Yuko Hirohata

Tel: +81-706-7108

Fax: +81-706-7108

e-mail address: [hirohta@qe.eng.hokudai.ac.jp](mailto:hirohta@qe.eng.hokudai.ac.jp)

Postal address: Graduate School of Engineering, Division of Quantum Science and Engineering, Hokkaido University, Kita-13, Nishi-8, Kita-ku, Sapporo, 060-8628 Japan

### Abstract

Helium irradiation experiments of V-4Cr-4Ti alloy with various surface treatments were conducted in an Electron Cyclotron Resonance (ECR) ion irradiation apparatus. After helium ion irradiation at room temperature, the helium thermal desorption and retention properties were examined by thermal desorption spectroscopy (TDS). Ion energy of helium beam was 5 keV. Three groups of desorption peaks appeared at around 500, 850 and 1200 K in the TDS spectrum. After helium ion irradiation at ion fluence of  $1 \times 10^{21}$  He/m<sup>2</sup>, the retained helium desorbed mainly at around 1200 K and all of the implanted helium atoms were retained. With increasing fluence up to  $5 \times 10^{21}$  He/m<sup>2</sup>, the amount of helium desorbed at 500 K increased. For the polished samples with annealing at various temperatures, the desorption peak observed at around 500 K shifted to higher temperature region. Smallest retained amount of helium was observed in the V-alloy with polishing followed by annealing at 1373 K.

Key words: vanadium alloy, ion irradiation, helium, thermal desorption

### 1. Introduction

V-4Cr-4Ti alloy is a promising material for fusion reactors [1-4] because it shows excellent mechanical tolerance to neutron damage [1,2] and has low helium and hydrogen production rates during 14 MeV neutron irradiation [4]. A first wall of V-alloy

is exposed to helium ions and charge exchange helium with different energies during helium glow discharge cleaning and exposure to helium ash resulting from fusion reactions. Therefore, the interaction of helium with vanadium alloy is an important issue, because in particular the re-emission of retained helium into the plasma results in the dilution of the hydrogen isotope fuel density.

There are reports on helium retention properties for vanadium alloys irradiated by helium ions, but the fluence was low ( $\sim 10^{18}$  He/m<sup>2</sup>) [5]. In our previous study, helium retention properties of cold rolled V-4Cr-4Ti alloy after annealing at 1373 K was investigated as a function of helium ion fluence [6]. It was found that the total amount of retained helium in the V-alloy samples saturated at the fluence up to  $\sim 5 \times 10^{21}$  He/m<sup>2</sup> and the saturation level was approximately  $2.7 \times 10^{21}$  He/m<sup>2</sup>. It is well known that pre-existing traps, e.g. under-sized alloying elements or interface boundaries of fine size and helium-vacancy clusters, act as sinks for helium in the surface region of the alloys [5]. It was reported that the distribution of fine precipitates consisted of Ti-O-C complex in V-4Cr-4Ti alloy was drastically changed by the final annealing temperature, i.e. precipitates with high density were found at 973 K, but dissolved at 1373 K [7,8], and was also affected by impurity uptake during annealing. Therefore, the helium retention properties might be strongly affected by the impurity distribution, surface geometry and final annealing temperature.

In the present study, the helium thermal desorption and retention properties of V-4Cr-4Ti alloy samples with and without polishing, and with annealing at different temperatures were examined by using an ECR ion irradiation apparatus [9]. Irradiation by helium ions was performed on V-alloy at room temperature with high flux ( $\sim 10^{18}$  He/m<sup>2</sup>/s) and high fluences ( $1 \times 10^{21}$  and  $5 \times 10^{21}$  He/m<sup>2</sup>). These fluences correspond to 9.1 and 45 dpa which are comparable to the operating condition of a DEMO reactor. After that, the retained and desorbed helium was measured by TDS.

## 2. Experiments

Table 1 shows the pre-irradiation preparation procedure of samples used in this study. Cold rolled V-4Cr-4Ti samples with low impurity contents [10], NIFS-HEAT-2, prepared by National Institute for Fusion Science (NIFS), were used. The sample size was 25 mm  $\times$  5 mm  $\times$  0.25 mm. Four kinds of V-alloy samples with various surface treatments were prepared. Sample 1 and 2 were prepared by only annealing of the cold rolled sample at 1373 K for 1 hr in the vacuum ( $\sim 10^{-5}$  Pa) of the ECR apparatus to re-dissolve the impurities and remove dislocations introduced by cold rolling. Sample 3 was polished and then annealed at the same condition of the sample 1. Sample 4 was

uniformly annealed in the vacuum of  $<10^{-4}$  Pa at 1373 K for 1 hr by using an infrared image furnace (HT apparatus), and then polished. Sample 5 was annealed finally at 973 K after the heating at 1373 K in the HT apparatus, and then polished. In the HT apparatus of NIFS, sample 4 and 5 wrapped with Zr getter foil were annealed to avoid the uptake of impurity (oxidation) during the annealing [8]. Sample 3, 4 and 5 were mechanically polished by using diamond paste containing  $\text{Al}_2\text{O}_3$  powder (0.05  $\mu\text{m}$ ) after rough polishing with emery paper #2000, and then were electro-polished in a solution of 20%  $\text{H}_2\text{SO}_4$ -80%  $\text{CH}_3\text{OH}$  [8]. Sample 4 and 5 were kept in methanol until He ion irradiation experiment to avoid the uptake of impurity from the atmosphere.

All the samples were irradiated by helium ions with energy of 5 keV at room temperature. The irradiated area was  $10^{-4}$   $\text{m}^2$ . The base pressure and the helium pressure during ion irradiation of the irradiation chamber were about  $10^{-6}$  Pa and  $9 \times 10^{-4}$  Pa, respectively. The helium ion flux was about  $1 \times 10^{18}$   $\text{He}/\text{m}^2\text{s}$  ( $\sim 9 \times 10^{-3}$  dpa/s). The fluence of helium ions was  $1 \times 10^{21}$   $\text{He}/\text{m}^2$  except sample 2 ( $5 \times 10^{21}$   $\text{He}/\text{m}^2$ ) corresponding to 9.1 dpa in the projected range (27 nm) of 5keV-He ion for pure vanadium. After helium ion irradiation, the sample was resistively heated from RT to 1600 K with a heating rate of 1 K/s in the ECR apparatus. The helium signal intensity of a quadrupole mass spectrometer (QMS) was calibrated by using a standard He leak, and then the retained amount of helium was quantitatively obtained by integrating the desorption rate of helium over the heating time.

The surface atomic composition and the change of surface morphology owing to the helium ion irradiation were examined by ex-situ Auger electron spectroscopy (AES) with 3keV-Ar ion etching and scanning electron microscopy (SEM), respectively.

### **3. Results and discussion**

#### **3.1. Depth profile of atomic composition and surface morphology**

Fig. 1 shows the depth profile of the atomic composition of the cold rolled sample (Fig. 1a), and sample 3 (Fig. 1b), Sample 5 (Fig. 1c) and Sample 3 after helium ion irradiation ( $1 \times 10^{21}$   $\text{He}/\text{m}^2$ ) (Fig. 1d). The depth was estimated by using the sputtering yield of pure vanadium of 3 keV Ar ion [11]. Carbon and oxygen with high content were contained in the near surface region of the cold rolled sample (Fig.1a). However, carbon and oxygen concentrations drastically decreased by annealing at 1373 K after polishing (Fig.1b Sample 3). Detail shapes of the AES spectrum of carbon shows the formation of carbides in the depth of  $>3$  nm, i.e. vanadium and/or titanium carbides. In addition, it was also found that titanium was segregated in the near surface region (surface concentration of Ti was about 20 at.%) in the form of oxide [12]. Similar

results were observed in both the sample 1 and 2 with annealing at 1373 K. The depth of the Ti-oxide layer was approximately 5 nm. The reduction of carbon and the segregation of Ti mainly occurred during annealing in vacuum. Although sample 5 was finally annealed at 973 K, carbon and oxygen with high concentration were observed and no Ti segregated layer was observed (Fig.1c). The latter indicates that the Ti-segregated layer produced by annealing was eliminated by the polishing. This impurity layer is related to methanol, because the fragment ion of methanol,  $\text{CH}_2\text{OH}^+$ , was detected during TDS measurements of sample 5 and 4. After helium ion irradiation, a Ti segregated layer with the thickness of 5 nm was sputtered. (Fig.1d). It can be seen that carbon concentration was very high and was almost constant (~20~30 at.%) beyond the depth of ~10 nm for all samples. Similar results were observed in V-4Cr-4Ti alloy samples produced by GA [13] and NIFS-HEAT1 [12] by both AES and XPS analyses. Since  $\text{Ar}^+$  ion etching was interrupted during measurements of AES and XPS spectra, residual gases might be adsorbed on the surface resulting in high impurity concentration. An additional AES measurement for sample 1 was carried out by changing the flow rate of Ar. It was found that carbon concentration drastically decreased below to 10 at.% by increasing Ar flow rate, but the small content of carbon was still remained, while oxygen was negligible. These results imply that sputtered C might be re-deposited (re-adsorbed) on the surface at lower Ar flow rate. For high carbon concentration, three reasons were suspected, i.e. (1) adsorption of residual gases, (2) re-deposition of sputtered C and (3) contained C in the near surface region. Therefore, carbon concentrations in the bulk would be significantly lower than those presented in Fig.1.

Fig. 2 shows SEM photographs of samples 3 (Fig. 2a), 5 (Fig. 2b) and 2 (Fig. 2c) after the He ion irradiation. Blisters with the size of  $<0.2 \mu\text{m}$  were observed on sample 3. The distribution of the blisters was not uniform and the density of the blisters was low,  $<2 \times 10^{11}/\text{m}^2$ . A lot of blisters with the size of  $0.1\sim 0.3 \mu\text{m}$  were observed on sample 5 even if the helium ion fluence was the same as that of the sample 3. The density of blisters on the sample 5 was  $\sim 10^{13}/\text{m}^2$ , which was two orders of magnitude larger than sample 3. Since sample 5 was polished after annealing and then kept in methanol, the impurities (C, O) with high concentration were deposited in the near surface region,. By this reason a lot of incident He was trapped in sample 5. With increasing fluence (sample 2), the density and size of blisters largely increased,  $3 \times 10^{13}/\text{m}^2$  and  $0.1\sim 0.5 \mu\text{m}$ . In the previous study, we found that after the heating at 673 K, no significant changes were observed in the surface of the sample 2, but, after the heating at 1473 K, a lot of blisters ruptured and a lot of pinholes was observed [6].

### 3.2 Thermal desorption and retention properties of helium

The thermal desorption spectra of helium of all the samples in the temperature range of  $\leq 1600$  K are shown in Fig.3a. Enlarged TDS spectra are also shown in Fig.3b. Several desorption peaks were observed in the TDS spectra (Fig.3a). These peaks were divided into three groups. Peak I was the desorption around 500 K, Peak II at 850 K, and Peak III at temperature higher than 1100 K. In our previous study, we determined that Peak I corresponds to the dissociation of  $\text{He}_n\text{VX}$  type defect clusters, Peak II to that of  $\text{He}_n\text{V}_5\text{X}$  clusters and Peak III to the rupture of blisters and internal bubbles with different size [5,6]. Here,  $n$  denotes the number of helium atom ( $n>1$ ), V vacancy, and X impurity atoms such as C, N or O. Peak III had multiple peaks corresponding to the rupture of blisters and bubbles with different size. It can be seen that at least two desorption peaks are contained in Peak I, and these desorption temperatures of the sample 3, 4 and 5 with polishing shifted to higher temperature region than without polishing (sample 1 and 2 (Fig. 3 (b))). This means that helium atoms are implanted deeper and  $\text{He}_n\text{VX}$  defects with large number of helium might be produced in the smooth surfaces, compared with those of rough surfaces. It seems that the amount of desorbed helium corresponding with the Peak I for sample 4 and 5 became large compared with sample 1 and 3. Fig. 4 shows the amount of desorbed helium for Peak I, II and III and the fraction of Peak I to the total amount of retained helium. The smallest retained amount was observed in sample 3 with annealing after polishing. For the samples 4 and 5 with polishing after annealing, the fraction of Peak I became 5~6 times larger than those of samples 1 and 3. One possible reason for large fraction of Peak I and large total retained amount was that the impurities were produced in sample 4 and 5 by the polishing after annealing. Although the number of precipitates of sample 5 (final annealing temperature ( $T_{\text{final}}$ ) =973 K) is much larger than sample 4 ( $T_{\text{final}}$  =1173 K) [7,8], the total amount of helium retained in sample 5 was rather smaller than sample 4. It means that the effect of polishing after annealing, i.e. impurity uptake and elimination of Ti-segregated layer, on He trapping is so strong that the differences in treatment prior to the polishing disappeared.

In addition, surprisingly, the total retention amount is higher than those of implanted helium atoms ( $1 \times 10^{21}$  He/m<sup>2</sup>). This excess retention was reproducibly observed in another sample 4. One possible explanation is that the surface with high impurity concentration results in an underestimation of helium ion fluence. However no experimental evidence for the difference of ion fluence between clean and oxidized surfaces has been reported. With an increase of the helium ion fluence (Sample 2), the fraction of Peak I increased. In addition, a lot of blistering was observed on sample 5.

These results imply that the fluence of samples 4 and 5 is also underestimated. Nevertheless this remains as an opened question.

#### **4. Conclusion**

The helium thermal desorption behavior and retention of V-4Cr-4Ti alloy with various surface treatments after ion implantation was investigated by TDS. A lot of blisters with a diameter of 0.1~0.5  $\mu\text{m}$  were observed after helium irradiation at room temperature. The density of the blistering changed with the surface treatment of the sample and the He ion fluence. Thermal desorption of helium due to the rupture of the blisters and internal bubbles was observed at the same temperature in all the samples. The peak temperature of helium at around 500 K for the sample with polishing shifted to higher temperature region. The amount of retained helium in the samples with the annealing was strongly affected by the carbon contamination.

Desorption and retention behaviors of helium examined in this study could be useful for wall conditioning of the first wall of a V-alloy blanket.

In order to investigate the effect of final annealing temperatures, further experiments are necessary by using samples without surface contamination at lower ion fluence (<100% trapping).

#### **Acknowledgements**

This study was supported by a Grant-in-Aid for Scientific Research (c), KAKENHI(16560719), by Japan Society for the Promotion of Science (JSPS), and also by Fusion Engineering Research Center in NIFS Collaboration Study.

#### **References**

- [1] S.J. Zinkle, H. Matsui, et.al., Research and development on vanadium alloys for fusion applications, *J.Nucl.Mater.* 258-263 (1998) 205-214.
- [2] D.L. Smith, H.M. Chung, et.al., Reference vanadium alloy V-4Cr-4Ti for fusion applications, *J.Nucl.Mater.* 233-237 (1996) 356-363.
- [3] T. Muroga, T. Nagasaka, et.al., Vanadium alloys-overview and recent results, *J.Nucl.Mater.* 307-311 (2002) 547-554.
- [4] D.L. Smith, M.C. Billone, et.al., Vanadium base alloys for fusion first-wall/blanket applications, *Interl.J. Refractory Metals & Hard Materials.* 18 (2000) 213-224.
- [5] A.V. Fedorov, A.van Veen, et.al., Helium vacancy clustering in V-4Cr-4Ti at elevated temperatures, *J.Nucl.Mater.* 258-263 (1998) 1396-1399.
- [6] Y. Hirohata, T. Yamada, et.al., Deuterium and helium retention of V-4Cr-4Ti alloy

used for first wall of breeding blanket in a fusion reactor, to be submitted in J.Nucl.Mater.

[7] A. Nishimura, A. Iwahori, et.al., Effect of precipitation and solution behavior of impurities on mechanical properties of low activation vanadium alloy, J.Nucl.Mater. 329-333 (2004) 438-441.

[8] N.J.Heo, T.Nagasaka, T.Muroga, H.Matsui, Effect of impurity levels on precipitation between the low-activation V-4Cr-4Ti alloys, J.Nucl.Mater. 307-311 (2002) 620-624.

[9] Y. Yamauchi, T. Hino, et.al., Hydrogen retention properties of low Z and high Z plasma facing materials, J.Nucl.Mater. 241-243 (1997) 1016-1021.

[10] T. Muroga, T. Nagasaka, et.al., NIFS program for large ingot production of a V-Cr-Ti alloy, J.Nucl.Mater. 283-287 (2000) 711-715.

[11] N. Matsunami, Y. Yamamura, et.al., Energy dependence of ion-induced sputtering yields of monatomic solids, At data, Nucl. Data table 31 (1) (1984) 26.

[12] Y. Yamauchi, T. Yamada, Y. Hirohata, et.al., Deuterium retention in V-4Cr-4Ti alloy after deuterium ion irradiation, J.Nucl.Mater. 329-333 (2004) 397-400.

[13] Y. Hirohata, T. Oda, T. Hino, S. Sengoku, Deuterium retention of V-4Cr-4Ti alloy exposed to the JFT-2M tokamak environment, J.Nucl.Mater. 290-293 (2001) 3196-200.

## Table contents and figures captions

Table 1 Sample pre-irradiation preparation procedure

Fig.1 Depth profiles of atomic composition of the cold rolled sample (a), sample 3 (b), sample 5 (c) and sample 3 after helium ion irradiation ( $1 \times 10^{21}$  He/m<sup>2</sup>).

Fig.2 SEM photographs of sample 3 (a), sample 5 (b) and sample 2 (c) after helium ion irradiation. The helium ion fluence of sample 3 and 5 is  $1 \times 10^{21}$  He/m<sup>2</sup>, and sample 2 is  $5 \times 10^{21}$  He/m<sup>2</sup>.

Fig.3 Thermal desorption spectra of helium of all the samples irradiated at room temperature with energy of 5 keV (a) and enlarged TDS spectra (b).

Fig.4 Desorbed helium for Peak I, II and III and the fraction of Peak I to total amount of retained helium.

Table 1 Sample pre-irradiation preparation procedure

	Sample 1	Sample 2	Sample 3	Sample 4	Sample 5
Pre-treatment procedure	Annealing 1373K, 1hr (in ECR <sup>**</sup> )		Polishing MP+EP* Annealing 1373K, 1hr (in ECR <sup>**</sup> )	Annealing 1373K, 1hr (in HT <sup>***</sup> ) Polishing MP+EP*	Annealing 1373K, 1hr Annealing 973K, 1hr (in HT <sup>***</sup> ) Polishing MP+EP*
Fluence (He/m <sup>2</sup> )	1x10 <sup>21</sup>	5x10 <sup>21</sup>	1x10 <sup>21</sup>	1x10 <sup>21</sup>	1x10 <sup>21</sup>

\*MP+EP: Sample was electro-polished after mechanical polishing

\*\*ECR: ECR ion irradiation apparatus, \*\*\*HT: Heat treatment apparatus

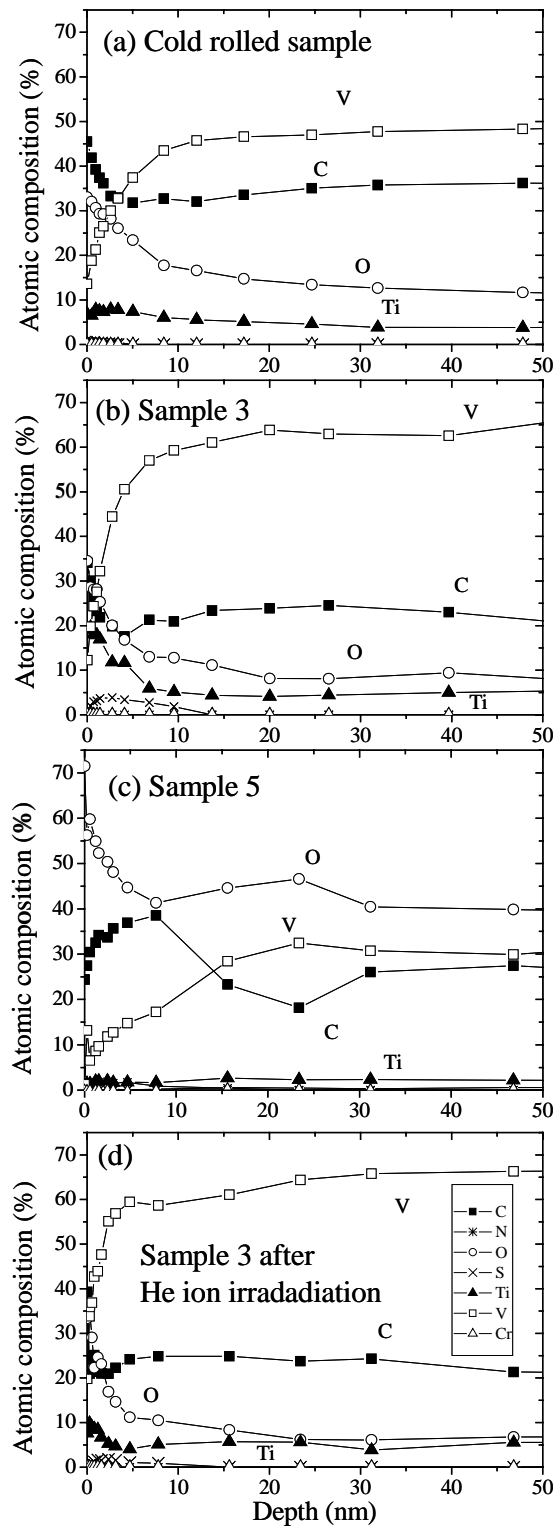
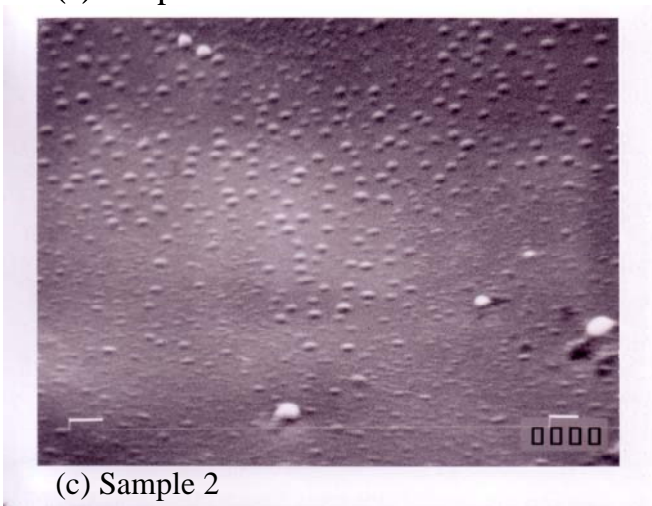


Fig.1 Hirohata

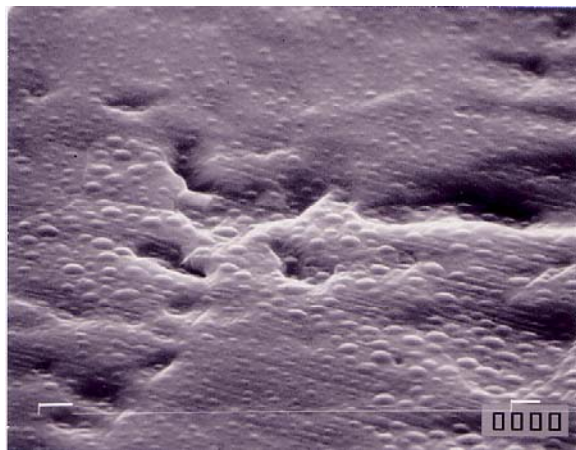
(a) Sample 3



(b) Sample 5



(c) Sample 2



←→  
5 μm

Fig.2 Hirohata

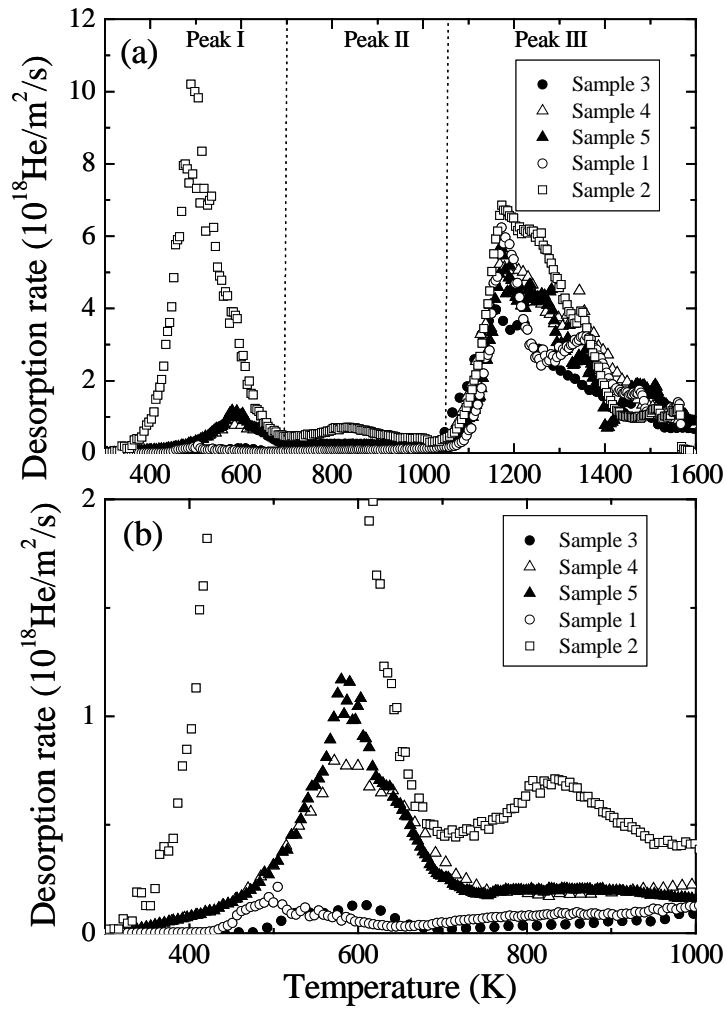


Fig.3 Hirohata

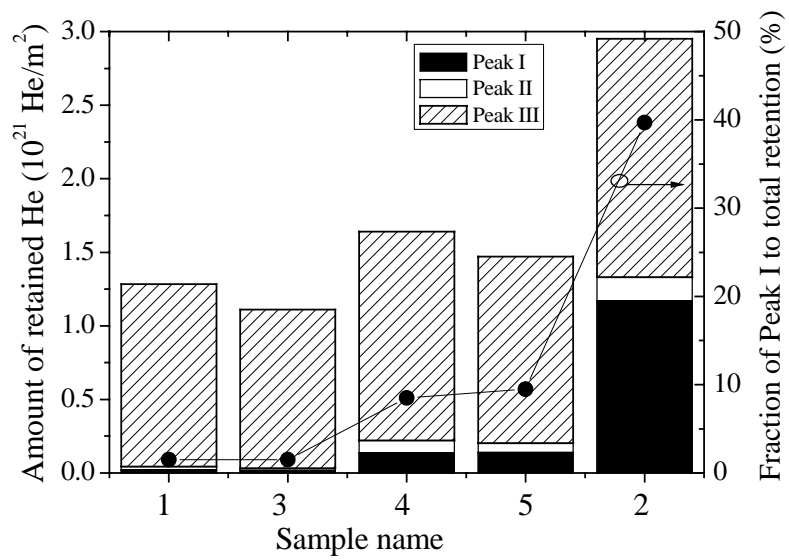


Fig.4 Hirohata